



# Support vector regression based shear strength modelling of deep beams

Mahesh Pal\*, Surinder Deswal

Department of Civil Engineering, NIT Kurukshetra, 136119 Haryana, India

## ARTICLE INFO

### Article history:

Received 27 November 2010

Accepted 17 March 2011

Available online 7 April 2011

### Keywords:

Support vector machines

Deep beam

Shear strength prediction

Strut-and-tie method

Back-propagation neural network

## ABSTRACT

Support vector regression based modelling approach was used to predict the shear strength of reinforced and prestressed concrete deep beams. To compare its performance, a back-propagation neural network and the three empirical relations was used with reinforced concrete deep beams. For prestressed deep beams, one empirical relation was used. Results suggest an improved performance by the SVR in terms of prediction capabilities in comparison to the empirical relations and back propagation neural network. Parametric studies with SVR suggest the importance of concrete cylinder strength and ratio of shear span to effective depth of beam on strength prediction of deep beams.

© 2011 Elsevier Ltd. All rights reserved.

## 1. Introduction

Various modelling approaches are being used to predict the behaviour of structures and their components by civil engineers. The traditional modelling approaches are based on empirical relationships derived using experimental data. Number of models has been proposed to predict the compressive strength and shear strength of beams and columns depending on different experimental conditions and assumptions. Several studies suggest the data specific nature of these models. As the design of a structure or a structural component may requires an iterative process in which the assumed model behaviour converges with the experimental behaviour, thus requiring a cost efficient computational technique.

Within last decade, researchers have explored the potential of back-propagation artificial neural networks (ANN) to solve various civil engineering problems. In structural engineering, neural networks have successfully been applied to several areas such as structural analysis and design [1–3], structural damage assessment [4–6], prediction of compressive strength of concrete mixes [7–18], shear strength prediction of reinforced concrete beams [19–24] and compressive strength of columns [25–28] as well as in non destructive strength assessment [29].

Determination of suitable architecture and various user-defined parameters has been a major issue in the design of an ANN [30]. ANN based modelling algorithm requires setting up of different learning parameters (like learning rate, momentum), the optimal number of nodes in the hidden layer and the number of hidden layers. In most of the reported applications, selection of number of hidden layers and the nodes in hidden layer is done by using

a rule of thumb or trying several arbitrary architectures to select one that gives the best performance with test dataset. A suitable value of parameters like learning rate and momentum is also required for selected hidden layers and nodes. Design of a back-propagation neural network also involves in using a non-linear optimisation problem that may results in a local minima. During training process a large number of training iterations may force ANN to over train, which may affect the predicting capabilities of the model. Several studies suggested using a validation dataset (i.e. a dataset other than the training dataset) to have an idea about the suitable number of iterations for a specific dataset. This may be a problem for studies where number of dataset is limited, like one of concrete strength prediction. Recent studies [31–33] suggest the usefulness of genetic algorithm to find the optimal architecture of ANN.

An alternative modelling technique, called Support Vector Machines [34], has recently been applied to the field of civil engineering and provides improved performance in comparison to empirical relations and back-propagation neural network [35–42]. Keeping in view the better performance by the support vector machines, present study examines its potential in predicting the shear strength of reinforced concrete deep beams and prestressed deep beams. The results obtained by the support vector machines were compared with the [43–44] codes and strut-and-tie methods. The results were also compared with a back-propagation neural network to highlight the efficiency of the proposed method.

## 2. Support Vector Regression (SVR)

Support vector machines are classification and regression methods, which have been derived from statistical learning theory [45]. The Support vector machines based classification methods is based

\* Corresponding author. Tel.: +91 1744 238353.

E-mail address: [mpce\\_pal@yahoo.co.uk](mailto:mpce_pal@yahoo.co.uk) (M. Pal).

**Nomenclature**

$a$	shear span of deep beam	$f_c$	concrete cylinder strength of reinforced deep beams
$A_s$	area of non-prestressed longitudinal steel reinforcement	$F_y$	yield strength of non-prestressed longitudinal steel reinforcement
$b_w$	web width of deep beams	$F_{pe}$	effective prestressing force after both immediate and long-term losses
$C$	regularization parameter	$F_c$	compressive force in concrete strut of prestressed deep beams
$D$	effective depth of beam	$V$	shear strength (in kN)
$D$	kernel specific parameters for polynomial kernel	$\rho_h$	ratio of horizontal web reinforcement
$h$	overall depth of prestressed deep beam	$\rho_s$	ratio of longitudinal reinforcement to area of concrete
$K$	kernel function	$\rho_v$	ratio of vertical web reinforcement
$L$	effective span of reinforced deep beams	$\gamma$	kernel specific parameter for RBF kernel
$f_{yh}$	yield strength of horizontal reinforcement		
$f_{yv}$	yield strength of vertical web reinforcement		

on the principle of optimal separation of classes. If the classes are separable – this method selects, from among the infinite number of linear classifiers, the one that minimise the generalisation error, or at least an upper bound on this error, derived from structural risk minimisation. Thus, the selected hyper plane will be one that leaves the maximum margin between the two classes, where margin is defined as the sum of the distances of the hyper plane from the closest point of the two classes [34].

Vapnik [34] proposed  $\varepsilon$ -Support Vector Regression (SVR) by introducing an alternative  $\varepsilon$ -insensitive loss function. This loss function allows the concept of margin to be used for regression problems. The purpose of the SVR is to find a function having at most  $\varepsilon$  deviation from the actual target vectors for all given training data and have to be as flat as possible [46]. For a given training data with  $k$  number of samples be represented by  $\{\mathbf{x}_i, y_i\}$ ,  $i = 1, \dots, k$ , where  $\mathbf{x}_i$  is input vector and  $y_i$  is the target value, a linear decision function can be represented by

$$f(\mathbf{x}) = \langle \mathbf{w}, \mathbf{x} \rangle + b \quad (1)$$

where  $\mathbf{w} \in \mathbf{R}^N$  and  $b \in \mathbf{R}$ .  $\langle \mathbf{w}, \mathbf{x} \rangle$  represents the dot product in space  $\mathbf{R}^N$ . In Eq. (1), vector  $\mathbf{w}$  determine the orientation of a discriminating plane whereas scalar  $b$  determine the offset of the discriminating plane from the origin. A smaller value of  $\mathbf{w}$  indicates the flatness of Eq. (1), which can be achieved by minimising the Euclidean norm defined by  $\|\mathbf{w}\|^2$  [34]. Thus, an optimisation problem for regression can be written as [46]:

$$\begin{aligned} &\text{minimise } \frac{1}{2} \|\mathbf{w}\|^2 \\ &\text{subject to } \begin{cases} y_i - \langle \mathbf{w}, \mathbf{x}_i \rangle - b \leq \varepsilon \\ \langle \mathbf{w}, \mathbf{x}_i \rangle + b - y_i \leq \varepsilon \end{cases} \end{aligned} \quad (2)$$

The optimisation problem in Eq. (2) is based on the assumption that there exists a function that provides an error on all training pairs which is less than  $\varepsilon$ . In real life problems, there may be a situation like one defined for classification by [47]. So, to allow some more error, slack variables  $\xi, \xi'$  can be introduced and the optimisation problem defined in Eq. (2) can be written as below to deal with infeasible constraints of the optimization problem (2) [46]:

$$\begin{aligned} &\text{Minimise } \frac{1}{2} \|\mathbf{w}\|^2 + C \sum_{i=1}^k (\xi_i + \xi'_i) \\ &\text{Subject to } y_i - \langle \mathbf{w}, \mathbf{x}_i \rangle - b \leq \varepsilon + \xi_i \\ &\langle \mathbf{w}, \mathbf{x}_i \rangle + b - y_i \leq \varepsilon + \xi'_i \end{aligned} \quad (3)$$

and  $\xi_i, \xi'_i \geq 0$  for all  $i = 1, 2, \dots, k$ .

The constant  $C > 0$  is a user-defined parameter which determines the trade-off between the flatness of the function and the

amount by which the deviations to the error more than  $\varepsilon$  can be tolerated. The minimization problem in Eq. (3) is called the primal objective function. It was found that that in most cases the optimization problem defined by Eq. (3) can easily be solved by converting it into a dual formulation [47]. The optimisation problem in Eq. (3) can be solved by replacing the inequalities with a simpler form determined by transforming the problem to a dual space representation using Lagrangian multipliers [48].

The Lagrangian of Eq. (3) can be formed by introducing positive Lagrange multipliers  $\lambda_i, \lambda'_i, \eta_i, \eta'_i$ ,  $i = 1, \dots, k$  and multiplying the constraint equations by these multipliers, and finally subtracting the results from the objective function (i.e.,  $\|\mathbf{w}\|^2$ ). The Lagrangian for Eq. (3) can now be written as:

$$\begin{aligned} L = & \frac{1}{2} \|\mathbf{w}\|^2 + C \sum_{i=1}^k (\xi_i + \xi'_i) - \sum_{i=1}^k \lambda_i (\varepsilon + \xi_i - y_i + \langle \mathbf{w}, \mathbf{x}_i \rangle + b) \\ & - \sum_{i=1}^k \lambda'_i (\varepsilon + \xi'_i + y_i - \langle \mathbf{w}, \mathbf{x}_i \rangle - b) - \sum_{i=1}^k (\eta_i \xi_i + \eta'_i \xi'_i) \end{aligned} \quad (4)$$

The dual variables in Eq. (4) have to satisfy  $\lambda_i, \lambda'_i, \eta_i, \eta'_i \geq 0$ . The solution of the optimisation problem involved in the design of SVR can be obtained by locating the saddle point of the Lagrange function defined in Eq. (4). The saddle points of Eq. (4) can be obtained by equating partial derivative of  $L$  with respect to  $\mathbf{w}$ ,  $b$ ,  $\xi_i$  and  $\xi'_i$  to zero and getting:

$$\partial_{\mathbf{w}} L = \mathbf{w} - \sum_{i=1}^k (\lambda'_i - \lambda_i) \cdot \mathbf{x}_i = 0 \quad (5)$$

$$\partial_b L = \sum_{i=1}^k (\lambda'_i - \lambda_i) = 0 \quad (6)$$

$$\partial_{\xi_i} L = C - \lambda_i - \eta_i = 0 \quad (7)$$

$$\partial_{\xi'_i} L = C - \eta'_i - \lambda'_i = 0 \quad (8)$$

Substituting Eqs. (5)–(8) in Eq. (4), results in the optimisation problem of maximizing:

$$\begin{aligned} & -\frac{1}{2} \sum_{i=1}^k \sum_{j=1}^k (\lambda'_i - \lambda_i)(\lambda'_j - \lambda_j)(\mathbf{x}_i \cdot \mathbf{x}_j) - \varepsilon \sum_{i=1}^k (\lambda'_i + \lambda_i) + \sum_{i=1}^k y_i (\lambda'_i - \lambda_i) \end{aligned} \quad (9)$$

$$\text{subject to } \sum_{i=1}^k (\lambda'_i - \lambda_i) = 0 \text{ and } \lambda_i, \lambda'_i \in [0, C]$$

Dual variables  $\eta_i, \eta'_i$  are eliminated by using conditions in Eqs. (7) and (8) and can now be written as  $\lambda'_i = C - \eta'_i$  and  $\lambda_i = C - \eta_i$ ,

whereas Eq. (5) can be written as  $\mathbf{w} = \sum_{i=1}^k (\lambda'_i - \lambda_i) \mathbf{x}_i$ . Eq. (9) is a quadratic programming problem and can be solved to get the values of  $\lambda'_i$  and  $\lambda_i$ . The prediction problem in Eq. (1) can now be written as:

$$f(\mathbf{x}) = \sum_{i=1}^k (\lambda'_i - \lambda_i) \langle \mathbf{x}_i, \mathbf{x} \rangle + b \quad (10)$$

The techniques discussed above can be extended to allow for non-linear support vector regression by introducing the concept of the kernel function [34]. This is achieved by mapping the data into a higher dimensional feature space. By doing this, the training data are moved into a higher-dimensional feature space where the training data may be spread further apart and a larger margin may be found by performing linear regression in feature space. The regression problem in feature space can be written by replacing  $\mathbf{x}_i \cdot \mathbf{x}_j$  in Eq. (6) with  $\Phi(\mathbf{x}_i) \cdot \Phi(\mathbf{x}_j)$ . Thus, the optimisation problem of Eq. (9) can be written as:

$$\begin{aligned} \text{maximize} \quad & -\frac{1}{2} \sum_{i=1}^k \sum_{j=1}^k (\lambda'_i - \lambda_i)(\lambda'_j - \lambda_j) K(\mathbf{x}_i \cdot \mathbf{x}_j) - \varepsilon \sum_{i=1}^k (\lambda'_i + \lambda_i) \\ & + \sum_{i=1}^k y_i (\lambda'_i - \lambda_i) \\ \text{subject to} \quad & \sum_{i=1}^k (\lambda'_i - \lambda_i) = 0 \text{ and } \lambda_i, \lambda'_i \in [0, C] \end{aligned} \quad (11)$$

where

$$K(\mathbf{x}_i, \mathbf{x}_j) \equiv \Phi(\mathbf{x}_i) \cdot \Phi(\mathbf{x}_j) \quad (12)$$

This relation is also called the kernel trick since no calculation of the mapping  $\Phi(\mathbf{x})$  is required in the feature space. Support vector regression function in Eq. (10) can now be written as:

$$f(\mathbf{x}) = \sum_{i=1}^k (\lambda'_i - \lambda_i) K(\mathbf{x}_i, \mathbf{x}) + b \quad (13)$$

In this optimisation problem, the kernel function is computed rather than  $\Phi(\mathbf{x})$  so as to reduce the computational cost of dealing with the high dimension feature space. For further details about SVR, readers are referred to [34,45].

### 3. Dataset used

To assess the effectiveness of SVR for shear strength prediction, data for reinforced as well as prestressed deep beams was used. All the data used in the present study was taken from the reported studies. The experimental data includes 106 reinforced and 30 prestressed deep beam results. The dataset for reinforced deep beams consists of 19 test results of high strength reinforced concrete from

[49], 52 test results from [50] and 35 test results from [51] of normal reinforced concrete. A brief detail of all datasets for reinforced deep beams is given in Table 1 and full dataset of 106 samples is provided in Table 2. For the dataset used in this study, the unit of shear strength is kN.

For prestressed deep beams, a dataset of 19 test results of simply supported unbounded post-tensioned deep beams from a study by Teng et al. [52] and another dataset consisting of 11 test results of post-tensioned deep beams by Tan et al. [53] were used. All specimens used by Teng et al. [52] have a height of 600 mm with support bearing plates of 100 mm. Dataset by Tan et al. [53] consists of specimens with height varying from 500 to 1750 mm while the ratio of shear span to effective depth of deep beams vary from 0.56 to 1.14. The width of the bearing plates with all 11 experiments was 150 mm. Detailed description of both datasets is available in [54] and provided in Table 3.

To predict the shear strength of reinforced deep beams with SVR, input parameter includes ratio of effective span to effective depth of beams ( $L/d$ ), concrete cylinder strength ( $f_c$ ), ratio of effective depth to breadth of beam ( $d/b_w$ ), ratio of shear span to effective depth of beam ( $a/d$ ), yield strength of horizontal reinforcement ( $f_{yh}$ ), yield strength of vertical web reinforcement ( $f_{yv}$ ), ratio of horizontal web reinforcement ( $\rho_h$ ), ratio of longitudinal reinforcement to area of concrete ( $\rho_s$ ) and ratio of vertical web reinforcement ( $\rho_v$ ) while shear strength ( $V$ ) was used as the output.

In case of prestressed deep beams the input parameters were length of beam ( $L$ ), overall depth of deep beam ( $h$ ), web width ( $b_w$ ), shear span ( $a$ ), effective depth of beam ( $d$ ), area of non-prestressed longitudinal steel reinforcement ( $A_s$ ), yield strength of non-prestressed longitudinal steel reinforcement ( $F_y$ ), effective prestressing force after both immediate and long-term losses ( $F_{pe}$ ) and compressive force in concrete strut ( $F_c$ ) while nominal shear strength ( $V_n$ ) was used as output parameter.

Several approaches are being used to design the deep beams. American Concrete Institute (ACI) code [43] based design approach is based on adding concrete contribution to the shear reinforcement contribution obtained by truss model, where concrete contribution is based on the experimental results. Several authors [55–59] reported the use of strut-and-tie method based design for deep beams. Strut-and-tie method is based on the assumption that compressive forces are carried by concrete struts while tensile forces are carried by steel reinforcement. Canadian Standards Association code [60] and the CEB-FIP MC90 [44] code also employ the strut-and-tie method. To compare the performance of SVR based shear strength prediction of deep beams, results obtained by strut-and-tie methods developed by Tan et al. [54] and Tang and Tan [59] for prestressed and reinforced deep beams were used. Predictions for reinforced deep beams were also compared with those obtained by using ACI [43] as well as CEB-FIP MC90 [44] codes.

**Table 1**  
Details of different reinforced deep beam datasets.

Tan et al. [49]	Smith and Vantsiotis [50]	Kong et al. [51]
Two point loading Over all height = 500 mm (19.7 in.), effective depth = 463 mm Width of beams = 110 mm	Two point loading Over all height = 356 mm, Effective depth = 305 mm  Width of beams = 102 mm	Two point loading Effective span = 762 mm (30 inch), shear span $a=254$ mm Width of beams = 76 mm No. 6 bar as the longitudinal Reinforcement with $A_s = 287 \text{ mm}^2$ , $f_y = 287 \text{ MPa}$
Longitudinal steel percentage = 1.23% Percentage of shear reinforcement = 0.48%	No. 5 bars as longitudinal reinforcement, with $A_s = 600 \text{ mm}^2$ (0.93 in. <sup>2</sup> ), $f_y = 431 \text{ MPa}$ $F_{yy}$ and $F_{yH} = 483.5 \text{ MPa}$	
Roller bearing plates of $150 \times 200 \times 125 \text{ mm}$ $a/d = 0.27\text{--}2.70$	Bearing plates of $102 \times 102 \times 25 \text{ mm}$ $a/d = 1\text{--}2.8$	$a/d = 1.05\text{--}3.53$

**Table 2**

Reinforced deep beam dataset.

$L/d$	$d/b_w$	$a/d$	$f_c$	$f_{yh}$	$f_{yv}$	$\rho_h$	$\rho_s$	$\rho_v$	$V$
<i>19 High strength deep beam data from [49]</i>									
2.1500	4.2091	0.2700	0.0588	0.5048	0.3752	0.0000	0.0123	0.0048	675
3.2300	4.2091	0.2700	0.0516	0.5048	0.3752	0.0000	0.0123	0.0048	630
4.3000	4.2091	0.2700	0.0539	0.5048	0.3752	0.0000	0.0123	0.0048	640
5.3800	4.2091	0.2700	0.0573	0.5048	0.3752	0.0000	0.0123	0.0048	630
2.1500	4.2091	0.5400	0.0560	0.5048	0.3752	0.0000	0.0123	0.0048	468
3.2300	4.2091	0.5400	0.0457	0.5048	0.3752	0.0000	0.0123	0.0048	445
4.3000	4.2091	0.5400	0.0539	0.5048	0.3752	0.0000	0.0123	0.0048	500
5.3800	4.2091	0.5400	0.0530	0.5048	0.3752	0.0000	0.0123	0.0048	480
2.1500	4.2091	0.8100	0.0512	0.5048	0.3752	0.0000	0.0123	0.0048	403
3.2300	4.2091	0.8100	0.0440	0.5048	0.3752	0.0000	0.0123	0.0048	400
2.1500	4.2091	1.0800	0.0482	0.5048	0.3752	0.0000	0.0123	0.0048	270
3.2300	4.2091	1.0800	0.0441	0.5048	0.3752	0.0000	0.0123	0.0048	280
4.3000	4.2091	1.0800	0.0468	0.5048	0.3752	0.0000	0.0123	0.0048	290
5.3800	4.2091	1.0800	0.0480	0.5048	0.3752	0.0000	0.0123	0.0048	290
3.2300	4.2091	1.6200	0.0506	0.5048	0.3752	0.0000	0.0123	0.0048	220
4.3000	4.2091	1.6200	0.0446	0.5048	0.3752	0.0000	0.0123	0.0048	190
5.3800	4.2091	1.6200	0.0453	0.5048	0.3752	0.0000	0.0123	0.0048	173
4.3000	4.2091	2.1600	0.0411	0.5048	0.3752	0.0000	0.0123	0.0048	150
5.3800	4.2091	2.7000	0.0428	0.5048	0.3752	0.0000	0.0123	0.0048	107
<i>52 Normal strength deep beam data from [50]</i>									
2.6700	2.9902	1.0000	0.0205	0.4835	0.4835	0.0000	0.0194	0.0000	140
2.6700	2.9902	1.0000	0.0209	0.4835	0.4835	0.0000	0.0194	0.0000	136
2.6700	2.9902	1.0000	0.0187	0.4835	0.4835	0.0023	0.0194	0.0028	161
2.6700	2.9902	1.0000	0.0180	0.4835	0.4835	0.0045	0.0194	0.0028	149
2.6700	2.9902	1.0000	0.0161	0.4835	0.4835	0.0068	0.0194	0.0028	141
2.6700	2.9902	1.0000	0.0206	0.4835	0.4835	0.0068	0.0194	0.0028	171
2.6700	2.9902	1.0000	0.0211	0.4835	0.4835	0.0091	0.0194	0.0028	184
2.6700	2.9902	1.0000	0.0217	0.4835	0.4835	0.0023	0.0194	0.0063	175
2.6700	2.9902	1.0000	0.0198	0.4835	0.4835	0.0045	0.0194	0.0063	171
2.6700	2.9902	1.0000	0.0203	0.4835	0.4835	0.0068	0.0194	0.0063	172
2.6700	2.9902	1.0000	0.0191	0.4835	0.4835	0.0091	0.0194	0.0063	162
2.6700	2.9902	1.0000	0.0181	0.4835	0.4835	0.0023	0.0194	0.0125	161
2.6700	2.9902	1.0000	0.0192	0.4835	0.4835	0.0045	0.0194	0.0125	173
2.6700	2.9902	1.0000	0.0208	0.4835	0.4835	0.0068	0.0194	0.0125	179
2.6700	2.9902	1.0000	0.0199	0.4835	0.4835	0.0091	0.0194	0.0125	168
3.0800	2.9902	1.2100	0.0217	0.4835	0.4835	0.0000	0.0194	0.0000	149
3.0800	2.9902	1.2100	0.0221	0.4835	0.4835	0.0023	0.0194	0.0024	148
3.0800	2.9902	1.2100	0.0201	0.4835	0.4835	0.0045	0.0194	0.0024	144
3.0800	2.9902	1.2100	0.0208	0.4835	0.4835	0.0068	0.0194	0.0024	141
3.0800	2.9902	1.2100	0.0195	0.4835	0.4835	0.0091	0.0194	0.0024	154
3.0800	2.9902	1.2100	0.0192	0.4835	0.4835	0.0023	0.0194	0.0042	129
3.0800	2.9902	1.2100	0.0190	0.4835	0.4835	0.0045	0.0194	0.0042	131
3.0800	2.9902	1.2100	0.0175	0.4835	0.4835	0.0068	0.0194	0.0042	126
3.0800	2.9902	1.2100	0.0218	0.4835	0.4835	0.0068	0.0194	0.0042	150
3.0800	2.9902	1.2100	0.0198	0.4835	0.4835	0.0091	0.0194	0.0042	145
3.0800	2.9902	1.2100	0.0162	0.4835	0.4835	0.0023	0.0194	0.0063	131
3.0800	2.9902	1.2100	0.0204	0.4835	0.4835	0.0023	0.0194	0.0077	159
3.0800	2.9902	1.2100	0.0190	0.4835	0.4835	0.0045	0.0194	0.0077	159
3.0800	2.9902	1.2100	0.0192	0.4835	0.4835	0.0068	0.0194	0.0077	155
3.0800	2.9902	1.2100	0.0207	0.4835	0.4835	0.0091	0.0194	0.0077	166
3.0800	2.9902	1.2100	0.0171	0.4835	0.4835	0.0023	0.0194	0.0125	154
3.6700	2.9902	1.5000	0.0207	0.4835	0.4835	0.0000	0.0194	0.0000	116
3.6700	2.9902	1.5000	0.0192	0.4835	0.4835	0.0023	0.0194	0.0018	119
3.6700	2.9902	1.5000	0.0219	0.4835	0.4835	0.0045	0.0194	0.0018	124
3.6700	2.9902	1.5000	0.0227	0.4835	0.4835	0.0068	0.0194	0.0018	131
3.6700	2.9902	1.5000	0.0218	0.4835	0.4835	0.0091	0.0194	0.0018	123
3.6700	2.9902	1.5000	0.0199	0.4835	0.4835	0.0023	0.0194	0.0031	124
3.6700	2.9902	1.5000	0.0192	0.4835	0.4835	0.0045	0.0194	0.0031	104
3.6700	2.9902	1.5000	0.0193	0.4835	0.4835	0.0045	0.0194	0.0031	116
3.6700	2.9902	1.5000	0.0204	0.4835	0.4835	0.0068	0.0194	0.0031	125
3.6700	2.9902	1.5000	0.0208	0.4835	0.4835	0.0091	0.0194	0.0031	124
3.6700	2.9902	1.5000	0.0210	0.4835	0.4835	0.0023	0.0194	0.0056	141
3.6700	2.9902	1.5000	0.0166	0.4835	0.4835	0.0045	0.0194	0.0056	125
3.6700	2.9902	1.5000	0.0183	0.4835	0.4835	0.0068	0.0194	0.0056	128
3.6700	2.9902	1.5000	0.0190	0.4835	0.4835	0.0091	0.0194	0.0056	137
3.6700	2.9902	1.5000	0.0196	0.4835	0.4835	0.0023	0.0194	0.0077	147
3.6700	2.9902	1.5000	0.0186	0.4835	0.4835	0.0045	0.0194	0.0063	129
3.6700	2.9902	1.5000	0.0192	0.4835	0.4835	0.0045	0.0194	0.0077	153
3.6700	2.9902	1.5000	0.0185	0.4835	0.4835	0.0068	0.0194	0.0077	153
3.6700	2.9902	1.5000	0.0212	0.4835	0.4835	0.0091	0.0194	0.0077	160
4.8300	2.9902	2.0800	0.0195	0.4835	0.4835	0.0000	0.0194	0.0000	74
4.8300	2.9902	2.0800	0.0161	0.4835	0.4835	0.0023	0.0194	0.0042	88

(continued on next page)

Table 2 (continued)

$L/d$	$d/b_w$	$a/d$	$f_c$	$f_{yh}$	$f_{yv}$	$\rho_h$	$\rho_s$	$\rho_v$	$V$
35 Normal strength deep beam data from [51]									
1.0500	9.5263	0.3500	0.0215	0.0000	0.2800	0.0000	0.0000	0.0245	239
1.2800	7.8553	0.4300	0.0246	0.0000	0.2800	0.0000	0.0000	0.0245	224
1.6200	6.1842	0.5400	0.0212	0.0000	0.2800	0.0000	0.0000	0.0245	190
2.2200	4.5132	0.7400	0.0212	0.0000	0.2800	0.0000	0.0000	0.0245	164
3.5300	2.8421	1.1800	0.0217	0.0000	0.2800	0.0000	0.0000	0.0245	90
1.0500	9.5263	0.3500	0.0192	0.0000	0.3030	0.0000	0.0000	0.0086	249
1.2800	7.8553	0.4300	0.0186	0.0000	0.3030	0.0000	0.0000	0.0086	224
1.6200	6.1842	0.5400	0.0199	0.0000	0.3030	0.0000	0.0000	0.0086	216
2.2200	4.5132	0.7400	0.0228	0.0000	0.3030	0.0000	0.0000	0.0086	140
3.5300	2.8421	1.1800	0.0201	0.0000	0.3030	0.0000	0.0000	0.0086	100
1.0500	9.5263	0.3500	0.0226	0.2800	0.0000	0.0245	0.0000	0.0000	276
1.2800	7.8553	0.4300	0.0210	0.2800	0.0000	0.0245	0.0000	0.0000	226
1.6200	6.1842	0.5400	0.0192	0.2800	0.0000	0.0245	0.0000	0.0000	208
2.2200	4.5132	0.7400	0.0219	0.2800	0.0000	0.0245	0.0000	0.0000	159
3.5300	2.8421	1.1800	0.0226	0.2800	0.0000	0.0245	0.0000	0.0000	87
1.0500	9.5263	0.3500	0.0220	0.3030	0.0000	0.0086	0.0000	0.0000	242
1.2800	7.8553	0.4300	0.0210	0.3030	0.0000	0.0086	0.0000	0.0000	201
1.6200	6.1842	0.5400	0.0201	0.3030	0.0000	0.0086	0.0000	0.0000	181
2.2200	4.5132	0.7400	0.0220	0.3030	0.0000	0.0086	0.0000	0.0000	110
3.5300	2.8421	1.1800	0.0226	0.3030	0.0000	0.0086	0.0000	0.0000	96
1.0500	9.5263	0.3500	0.0186	0.2800	0.2800	0.0061	0.0000	0.0061	240
1.2800	7.8553	0.4300	0.0192	0.2800	0.2800	0.0061	0.0000	0.0061	208
1.6200	6.1842	0.5400	0.0201	0.2800	0.2800	0.0061	0.0000	0.0061	173
2.2200	4.5132	0.7400	0.0219	0.2800	0.2800	0.0061	0.0000	0.0061	127
3.5300	2.8421	1.1800	0.0226	0.2800	0.2800	0.0061	0.0000	0.0061	78
1.0500	9.5263	0.3500	0.0261	0.3030	0.0000	0.0051	0.0000	0.0000	308
1.2800	7.8553	0.4300	0.0251	0.3030	0.0000	0.0061	0.0000	0.0000	266
1.6200	6.1842	0.5400	0.0261	0.3030	0.0000	0.0077	0.0000	0.0000	245
2.2200	4.5132	0.7400	0.0261	0.3030	0.0000	0.0102	0.0000	0.0000	173
3.5300	2.8421	1.1800	0.0251	0.3030	0.0000	0.0153	0.0000	0.0000	99
1.0500	10.0263	0.3500	0.0251	0.3030	0.0000	0.0000	0.0000	0.0000	253
1.0500	10.0263	0.3500	0.0261	0.3030	0.0000	0.0017	0.0000	0.0000	300
1.0500	10.0263	0.3500	0.0251	0.3030	0.0000	0.0034	0.0000	0.0000	260
1.0500	10.0263	0.3500	0.0213	0.3030	0.0000	0.0068	0.0000	0.0000	264
1.0500	10.0263	0.3500	0.0213	0.3030	0.0000	0.0085	0.0000	0.0000	297

Table 3  
Prestressed deep beams dataset.

$L$	$h$	$b_w$	$a$	$d$	$A_s F_y$	$F_{pe}$	$F_c$	$V_n$
19 Data from [52]								
1800	600	150	900	550	573	123.1	0.03843	290
1800	600	160	900	550	363	112.8	0.04009	214
1800	600	150	900	550	573	141.8	0.03839	412.5
1800	600	150	900	550	573	160.4	0.03845	425
1800	600	150	900	550	573	130.6	0.03845	437.5
1800	600	150	900	550	573	179.5	0.03835	460
1800	600	150	900	550	573	129.1	0.03843	275
1800	600	160	900	550	363	134.1	0.04009	287.5
1800	600	150	900	550	573	184	0.03831	375
1800	600	160	900	550	363	141.7	0.04013	318
1800	600	160	900	550	363	154.2	0.04824	295
1800	600	150	900	550	573	173.1	0.03848	367.5
1800	600	150	900	550	573	170.8	0.0385	475
1800	600	160	900	550	363	266.4	0.04338	370
1800	600	160	900	550	363	265.4	0.04347	437.5
1800	600	160	900	550	363	266.1	0.04354	400
1200	600	160	600	550	363	219.2	0.04318	417.5
1200	600	160	600	550	363	211.5	0.04328	537.5
1200	600	160	600	550	363	225.4	0.04331	560
11 Data from [53]								
1900	500	140	250	444	640	126.8	0.0466	815
2150	500	140	375	444	640	133.9	0.0427	590
2400	500	140	500	444	640	138.9	0.0393	450
2640	1000	140	500	884	1322	301.2	0.0435	1350
3120	1000	140	740	884	1322	301.9	0.0406	1200
3640	1000	140	1000	884	1322	336.9	0.0358	900
3210	1400	140	705	1251	2002	450	0.0348	1300
3900	1400	140	1050	1251	2002	472.2	0.0335	1250
4640	1400	140	1420	1251	2002	363.6	0.0395	950
4640	1750	140	1320	1559	2503	604.9	0.0383	1325
5520	1750	140	1760	1559	2503	662.3	0.0409	1100

#### 4. Details of SVR

As discussed in Section 2, in situations with non-linear decision surfaces, SVR use a mapping to project the data in a higher dimensional feature space. To make computation simpler, the concept of the kernel function was introduced [34]. A kernel function allows SVR to work in a high-dimensional feature space, without actually performing calculations in that space. Kernel functions are mathematical functions and according to [47], any symmetric positive semi-definite function, which satisfies Mercer's conditions [34], can be used as a kernel function with SVR. A number of kernel functions are discussed in the literature, but it is difficult to choose one which gives the best generalisation with a given dataset. As the choice of kernel function may influence the prediction capabilities of the SVR, two most frequently used kernel functions: a polynomial kernel function ( $K(\mathbf{x}, \mathbf{x}') = ((\mathbf{x} \cdot \mathbf{x}') + 1)^{d^*}$ ) and a radial basis kernel ( $K(\mathbf{x}, \mathbf{x}') = e^{-\gamma \|\mathbf{x} - \mathbf{x}'\|^2}$ ) were used in present study, where  $d^*$  and  $\gamma$  are the parameters of polynomial and radial basis kernel function, respectively. The use of SVR requires setting of user-defined parameters such as regularisation parameter ( $C$ ), type of kernel, kernel specific parameters and error-insensitive zone  $\varepsilon$ . Variation in error-insensitive zone  $\varepsilon$  found to have no effect on the predicted shear strength in present study so a default value of 0.0010 was chosen for all experiments [61]. The optimal value of parameters  $C$ ,  $d^*$  and  $\gamma$  were obtained after several trials with this dataset. The correlation coefficients and Root Mean Square Error (RMSE) were compared to reach at an optimal choice of these parameters.

Cross-validation is used to generate the model with SVR on the input dataset and predicting the shear strength of the datasets used in the study. The cross-validation is a method of estimating



the accuracy of a classification or regression model. The input dataset is divided into several parts (a number defined by the user), with each part in turn used to test a model fitted to the remaining parts. For this study, a tenfold cross-validation was used. The correlation coefficient and root mean square error (RMSE) was used to judge the performance of SVR in predicting the shear strength with different datasets used in present study. SVR software used in present study is based on sequential minimisation optimisation [62] as implemented in [61]. In this study, *smo\_poly* and *smo\_rbf* represents a polynomial and radial basis kernel function based implementation of SVR algorithm respectively.

## 5. Results and analysis

### 5.1. Reinforced deep beams

Table 4 provides the value of optimal value of user-defined parameters as well as the correlation coefficient and RMSE values obtained with reinforced deep beam data using both kernels. To compare the performance of different approaches, graphs between actual and predicted strength are plotted in a way to show the scatter around a line of perfect agreement (i.e. a line at 45°). The performance of SVR as well as ACI [43], CEB-FIP MC90 [44] and strut-and-tie methods is shown in Fig. 1. Results suggest effectiveness of SVR in predicting shear strength with this dataset as all of the points are lying within  $\pm 10\%$  of the line of perfect agreement (Fig. 1(a)). A correlation coefficient of 0.99 (RMSE = 20.9 kN) and 0.98 (RMSE = 23.78 kN) was achieved with polynomial and radial basis function kernels respectively (Table 4). In comparison to SVR, Fig. 1(b) suggests that the ACI [43], CEB-FIP MC90 [44] and the strut-and-tie method under-predict the shear strength for this dataset. The average ratio of actual to predicted strength of all specimens is 1.69, 1.74 and 1.28 with ACI method, CEB-FIP MC90 [44] and the strut-and-tie method of [54], respectively. In comparison, SVR based approach provides values of 1.006 and 1.013 with polynomial and radial basis kernel function, respectively.

Back-propagation neural network was used to compare the performance of SVR with this dataset. A large number of trials were carried out to find the suitable values of different user defined parameters (i.e. learning rate, momentum, number of hidden layers and nodes in each hidden layer as well as the number iterations). The optimal value of these parameters for the given dataset is provided in Table 5. The value of correlation coefficient, RMSE and average ratio of actual strength to predicted strength was 0.98, 23.1 kN and 0.99 for all specimens with this approach for reinforced concrete deep beam dataset. Fig. 1(c) provides a plot between actual and predicted strength values by back-propagation neural network with this dataset. A comparison of RMSE and correlation coefficient values (Tables 4 and 5) suggests better performance by polynomial based support vector machines in comparison to a back-propagation neural network with this dataset. As discussed in Section 1, several issues including local minima and large number of user defined parameters affects the performance of back-propagation neural network based modelling approach. In comparison, SVR is based on using a quadratic optimisation problem which provides global minima and require setting of only two user defined parameters for a given choice of kernel function. For comparison, computational cost (i.e. training

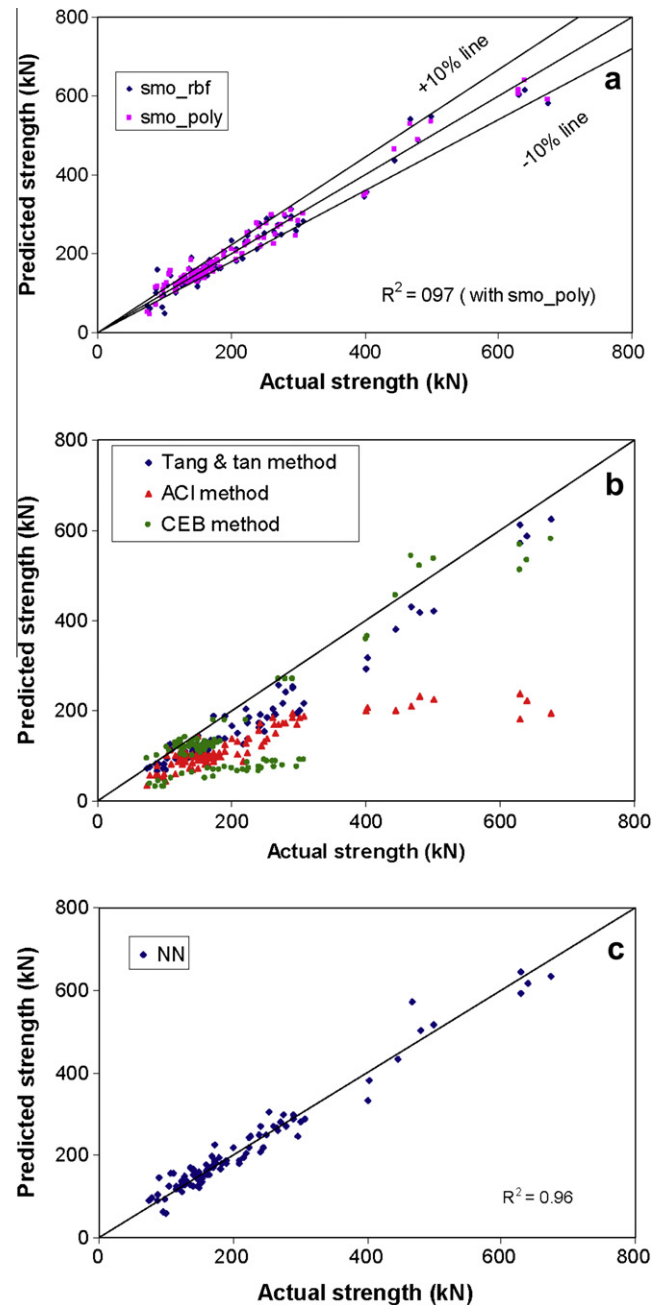


Fig. 1. Actual Shear strength versus predicted shear strengths (in kN) by different methods (a) SVR with both kernel functions (b) Tang and Tan, ACI and CEB-FIP MC90 methods and (c) back-propagation neural network.

and test time) of using SVR and back-propagation neural network with reinforced deep beam dataset was also obtained. In comparison to a time of 5.88 s by SVR, a back-propagation neural network requires 67.28 s on a Pentium-IV computer with 512 MB of RAM. Thus, suggesting effectiveness of SVR approach in terms of computational cost also.

Table 4

Correlation coefficient and root mean square error values as well optimal values of user defined parameters with reinforced deep beams using SVR.

	C	$\gamma$	smo_rbf		C	$d^*$	smo_poly	
			Correlation coefficient	Root mean square error			Correlation coefficient	Root mean square error
Strength prediction	20	0.3	0.98	23.78	20	2	0.99	20.90

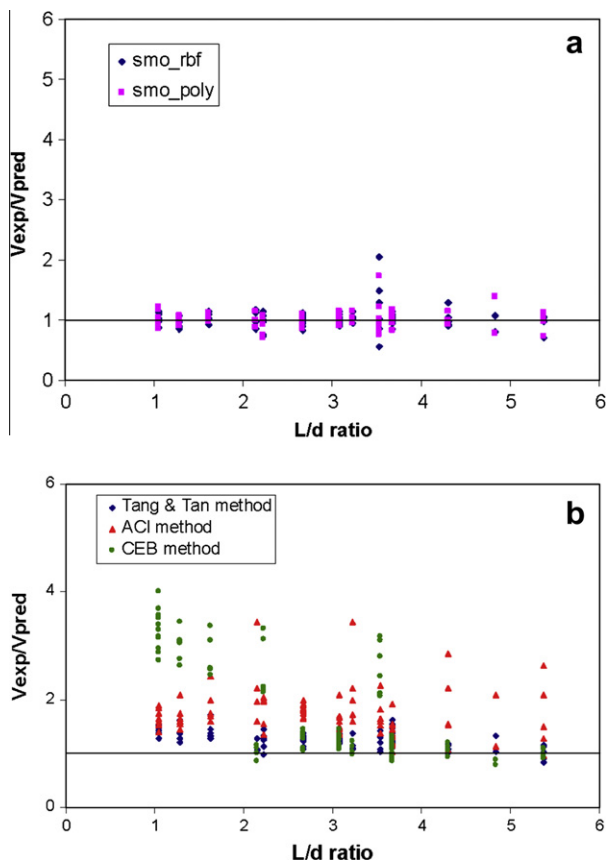
**Table 5**

Correlation coefficient and root mean square error values as well optimal values of user defined parameters with reinforced deep beams using back-propagation neural network.

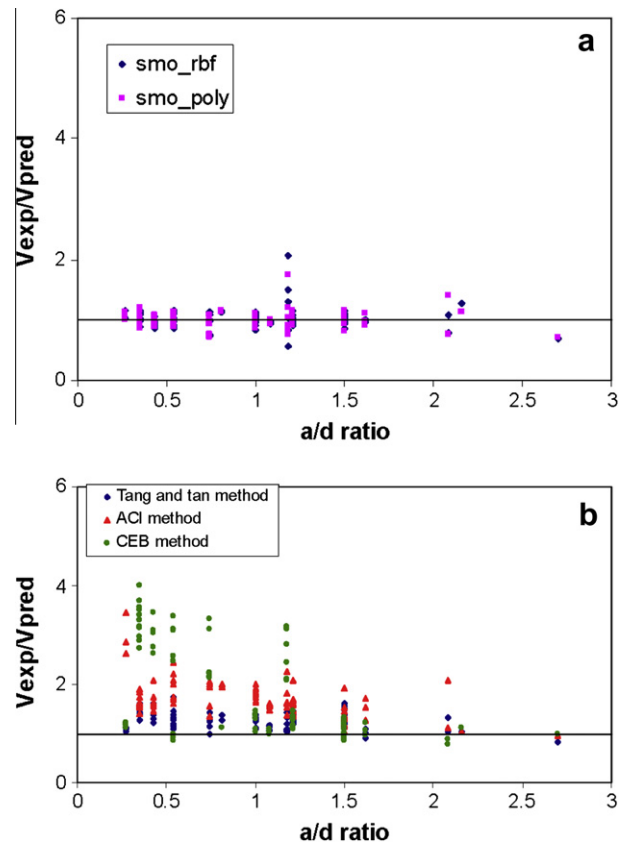
Hidden nodes	Momentum	Learning rate	Iterations	Correlation coefficient	Root mean square error
5	0.01	0.07	1000	0.98	23.10

Fig. 2 presents the variation of the ratio of actual to predicted strength with the  $L/d$  ratio. A large variation in the ratio of actual to predicted strength is obtained with ACI [43] and CEB-FIP MC90 [44] methods in comparison to the strut-and-tie method by Tan et al. [54]. A comparison of results with SVR suggests an improved performance by this approach in comparison to the ACI [43], CEB-FIP MC90 [44] codes and strut and Tie method by Tan et al. [54] in all ranges of the  $L/d$  ratios and most of the values are very close to 1. The variations of the ratio of actual strength to predicted strength with the  $a/d$  ratio for all three methods considered in this study are shown in Fig. 3. Results indicate a better performance by SVR for all ranges of  $a/d$  values considered in this study in comparison to ACI [43], CEB-FIP MC90 [44] codes and Strut and tie method.

The compressive strength of the concrete ( $f_c$ ) was plotted against the ratio of actual strength to predicted strength and shown in Fig. 4 for different modelling approaches. Result indicates that the strength predications by SVR are mostly unaffected by the variation in compressive strength of concrete and performs better than the ACI [43], CEB-FIP MC90 [44] codes and Strut and tie method.



**Fig. 2.** Variation of actual to predicted strength with  $L/d$  (a) SVR with both kernel functions (b) Tang and Tan, ACI and CEB-FIP MC90 methods.



**Fig. 3.** Variation of actual to predicted strength with  $a/d$  (a) SVR with both kernel functions (b) Tang and Tan, ACI and CEB-FIP MC90 methods.

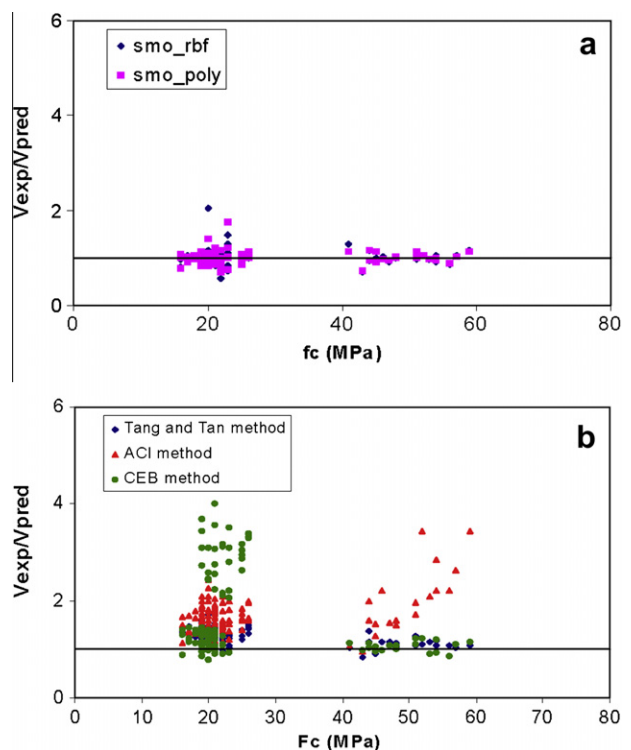


**Fig. 4.** Variation of actual to predicted strength with  $f_c$  (a) SVR with both kernel functions (b) Tang and Tan, ACI and CEB-FIP MC90 methods.

**Table 6**

Correlation coefficient and root mean square error values and user defined parameters with prestressed deep beams using SVR.

	C	$\gamma$	smo_rbf		C	$d^*$	smo_poly	
			Correlation coefficient	Root mean square error			Correlation coefficient	Root mean square error
Strength prediction	20	2	0.97	92.11	20	1	0.95	112.15

Figs. 2–4 indicate an improved performance by SVR based approach for deep beam strength prediction. Result with this dataset also suggests better performance by polynomial kernel in comparison to RBF kernel based SVR for this dataset.

## 5.2. Prestressed deep beams

Similar to simple reinforced deep beams, several trials were carried out to find the suitable choice of parameter C and kernel specific parameters for strength prediction of prestressed deep beams. Table 6 provides the value of user-defined parameters as well as the correlation coefficient and RMSE value obtained with prestressed deep beam data with both radial basis function and polynomial kernel function based SVR.

Fig. 5 shows the performance of SVR as well as the strut-and-tie method by Tan et al. [54] in predicting the shear strength for this dataset. Graph suggests that radial basis kernel function based SVR work well with this dataset as most of the points are lying within  $\pm 15\%$  of the line of perfect agreement (Fig. 5(a)). In comparison, Fig. 5(b) suggest that strut-and-tie method under predict the shear strength. The average ratio of actual to predicted strength of

all 30 data is 1.225 with the strut-and-tie method whereas radial basis and polynomial kernel function based SVR provides a value of 1.02 and 0.98, respectively. In contrast to the SVR performance with reinforced deep beams dataset radial basis kernel function perform better than the polynomial kernel function with this dataset.

## 6. Parametric study based on SVR results

Results in Section 5 suggest that SVR based modelling approach is capable of generalisation well within the range of the input parameters used in this study. This section discusses the influence of the different parameters which affect the shear strength of deep beams. This is achieved by testing the model created in Section 5.1 with hypothetical test data sets. The hypothetical test datasets are creating by varying one input parameter while keeping all other input parameters constant. In this section, two parametric studies, as discussed below, are carried out.

First parametric study consists in studying the effect of varying the shear span to effective depth ratio and concrete strength on the shear strength of reinforced deep beams (Fig. 6). This study is carried out by changing the value of concrete strength for a fixed value of  $a/d$  ratio, while other input parameters are kept constant. Four datasets having  $a/d$  values of 0.5, 1.0, 1.5 and 2.0 are used while  $f_c$  value is varied from 20 to 40 MPa for each value of  $a/d$  ratio. Fig. 6 shows that the variations of shear strength of a deep beam with varying  $f_c$  value and increasing  $a/d$  ratio. Same trends in variation of shear strength as suggested by Smith and Vantsiotis [50] are achieved by SVR based modelling approach.

Results of another parametric study involve in varying the amount of longitudinal steel ratio for a fixed value of transverse steel ratio and a fixed value of  $a/d$  (i.e. 0.25). All other data are kept constant in the hypothetical test dataset. Two datasets for different value of transverse steel ( $\rho_v = 0.24$  and 0.48) are used while longitudinal steel ( $\rho_h$ ) is varied from 0.54% to 0.76%. Fig. 7 present the results with this dataset by using the SVR model based on the dataset used in Section 5.1. Results show that SVR based approach provides the same trend as suggested by Smith and Vantsiotis [50] where increase in horizontal web reinforcement have little influence on the shear strength of beams for a given vertical web reinforcement.

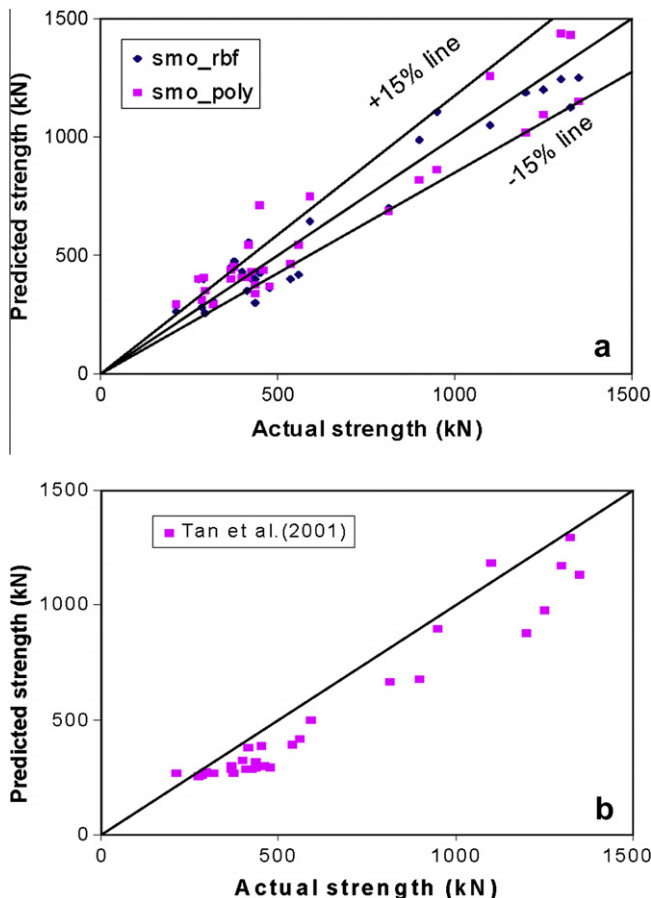


**Fig. 5.** Actual Shear strength versus predicted shear strengths (in kN) for prestressed deep beams (a) SVR with both kernel functions (b) [54].

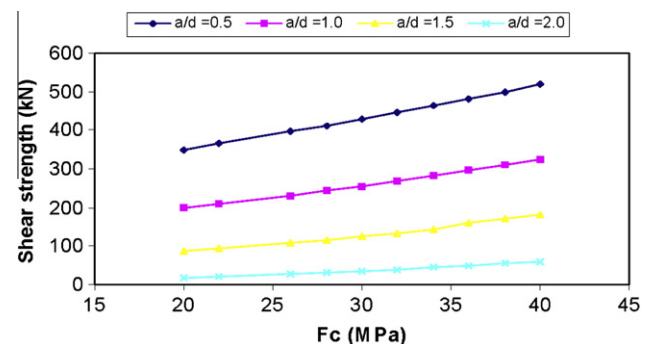


**Fig. 6.** Variation of shear strength with a fixed value of  $a/d$  and varying concrete strength.



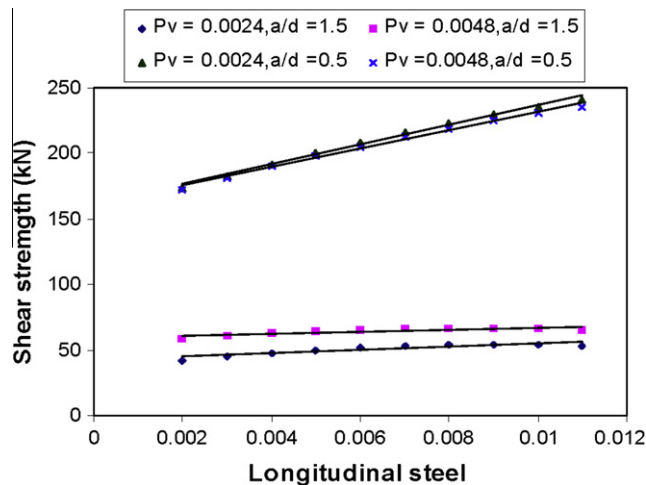


Fig. 7. Variation of shear strength with a fixed value of transverse steel with increasing amount of the longitudinal reinforcement.

Table 7  
Sensitivity analysis of input variables using SVR.

Input parameter combination	Correlation coefficient	Root mean square error	Computation cost (s)
$L/d, d/b_w, a/d, f_c, f_{yh}, f_{yy}, \rho_h, \rho_s, \rho_v$	0.99	20.90	5.88
$L/d, d/b_w, f_c, f_{yh}, f_{yy}, \rho_h, \rho_s, \rho_v$	0.92	47.75	2.38
$L/d, d/b_w, a/d, f_{yh}, f_{yy}, \rho_h, \rho_s, \rho_v$	0.98	27.08	3.86
$a/d, f_c, f_{yh}, f_{yy}, \rho_h, \rho_s, \rho_v$	0.98	26.46	1.69
$L/d, d/b_w, f_{yh}, f_{yy}, \rho_h, \rho_s, \rho_v$	0.72	84.55	1.89
$L/d, d/b_w, a/d, f_c$	0.98	25.91	0.34
$d/b_w, a/d, f_c$	0.95	39.46	0.30
$a/d, f_c$	0.93	45.32	0.16

## 7. Input parameter significance

This section discusses the use of SVR in judging the importance of different input parameters (i.e.  $L/d, d/b_w, a/d, f_c, f_{yh}, f_{yy}, \rho_h, \rho_s, \rho_v$ ) on the strength prediction of deep beams. An approach suggested by Sung and Mukkamala [63] to identify important features for a classification problem was used in this study to judge the importance of different input parameters on shear strength of deep beams. To rank different input features, the procedure involves in deleting one or more features from the dataset and using the resultant dataset to create and test the model by 10 fold cross-validation using polynomial kernel based SVR. Various input combinations as provided in Table 7 were considered by removing input variables and their influence on strength prediction was evaluated in terms of the RMSE, correlation coefficient and computational cost was used as main performance criteria. Results from Table 7 suggest that the concrete cylinder strength ( $f_c$ ) and ratio of shear span to effective depth of beam ( $a/d$ ) has major influence on the strength prediction of deep beams. However considering the limitations with the availability of the data, a model involving all inputs parameters would be desirable in spite of slightly higher computational cost.

## 8. Discussion of results

Results from this study suggest that SVR based modelling approach provides better results in comparison to the ACI and strut-and-tie methods. As the choice of a suitable architecture has always been a problem with neural network approach, results from this study suggests that SVR can be used as an alternative

modelling tool for shear strength prediction of deep beams. One major advantage of using SVR is the use of quadratic optimisation problem which provides global minima in comparison to the presence of local minima due to the use of a non-linear optimisation problem with a back-propagation neural network. With reinforced deep beams, proposed approach works quite well with polynomial kernel while it works well with radial basis kernel in case of pre-stressed deep beam data. Further, SVR uses data points closest to the hyperplane (called support vectors) in decision making, suggesting a better generalisation with small number of training data. This suggests a better performance can be achieved using SVR with smaller number of training data in comparison to back-propagation neural network approach. Thus SVR can effectively be used in modelling physical processes like one predicting the shear strengths of deep beams, within the range of input parameters used to train the model, rather than referring to costly experimental investigation.

## 9. Conclusions

This study suggests that SVR is a powerful computational tool and can effectively be used to analyse the complex relationship between various parameter used in predicting shear strength of deep beams. Comparisons between the SVR and strut-and-tie as well as ACI approaches indicate that SVR results are better. In spite of the fact that determination of C and kernel specific parameters still requires a heuristic process, this paper shows the potential of SVR with a suitable kernel function as an alternative modelling technique for shear strength predication of deep beams in place of back-propagation neural network and other empirical approaches.

The SVR model is also used to perform parametric studies and found to be successful in modelling physical processes. The parametric studies suggest that the shear strength of deep beams increases as the concrete strength increases and the shear span-to-depth-ratio decreases. The shear strength of deep beams is not affected by the variation in horizontal web reinforcement for  $a/d > 1$  while the influence of variation in horizontal web reinforcement on shear strength is more predominant for  $a/d < 1$ . The results of the parametric studies using SVR were in agreement with the work carried out by Smith and Vantsiotis [50].

## References

- [1] Hajela P, Berke L. Neurobiological computational models in structural analysis and design. *Comput Struct* 1991;41(4):657–67.
- [2] Consolazio GR. Iterative equation solver for bridge analysis using neural networks. *Comput Aided Civ Infrastr Eng* 2000;15(2):107–19.
- [3] Jenkins WM. A neural network for structural re-analysis. *Comput Struct* 1999;72(6):687–98.
- [4] Elkordy MF, Chang KC, Lee GC. Neural networks trained by analytically simulated damage states. *J Comput Civil Eng* 1993;7(2):130–45.
- [5] Mukherjee A, Deshpande JM, Annada J. Prediction of buckling load of columns using artificial neural networks. *J Struct Eng* 1996;122(11):1385–7.
- [6] Zhao J, Ivan JN, DeWolf JT. Structural damage detection using artificial neural network. *J Infrastruct Syst* 1998;4(3):93–101.
- [7] Kasperkiewicz J, Racz J, Dubrawski A. HPC strength prediction using artificial neural network. *J Comput Civil Eng* 1995;9(4):279–84.
- [8] Kim J, Kim DK, Feng MQ, Yazdani F. Application of neural networks for estimation of concrete strength. *J Mater Civil Eng* 2004;16(3):257–64.
- [9] Dias WPS, Pooliyadda SP. Neural networks for predicting properties of concretes with admixtures. *Construct Build Mater* 2001;15(7):371–9.
- [10] Lee S. Prediction of concrete strength using artificial neural networks. *Eng Struct* 2003;25(7):849–57.
- [11] Hong-Guang N, Ji-Zong W. Prediction of compressive strength of concrete by neural networks. *Cement Concrete Res* 2000;30(8):1245–50.
- [12] Yeh IC. Design of high-performance concrete mixture using neural networks and nonlinear programming. *J Comput Civil Eng* 1999;13(1):36–42.
- [13] Lai S, Serra M. Concrete strength prediction by means of neural network. *Construct Build Mater* 1997;11(2):93–8.
- [14] Ren LQ, Zhao ZY. An optimal neural network and concrete strength modeling. *J Adv Eng Software* 2002;33(3):117–30.
- [15] Özcan F, Atis CD, Karahan O, Uncuoglu E, Tanyildizi H. Comparison of artificial neural network and fuzzy logic models for prediction of long-term

- compressive strength of silica fume concrete. *Adv Eng Software* 2009;40(9):856–63.
- [16] Naderpour H, Kheyroddin A, Amiri GG. Prediction of FRP-confined compressive strength of concrete using artificial neural networks. *Compos Struct* 2010;92(12):2817–29.
- [17] Sobhani J, Najimi M, Pourkhorshidi AR, Parhizkar T. Prediction of the compressive strength of no-slump concrete: a comparative study of regression, neural network and ANFIS models. *Construct Build Mater* 2010;24(5):709–18.
- [18] Słonski M. A comparison of model selection methods for compressive strength prediction of high-performance concrete using neural networks. *Comput Struct* 2010;88(21–22):1248–53.
- [19] Sanad A, Saka MP. Prediction of ultimate shear strength of reinforced-concrete deep beams using neural networks. *J Struct Eng* 2001;127(7):818–28.
- [20] Cladera A, Mari AR. Shear design procedure for reinforced normal and high-strength concrete beams using artificial neural networks. Part I: beams without stirrups. *Eng Struct* 2004;26(7):917–26.
- [21] Cladera A, Mari AR. Shear design procedure for reinforced normal and high-strength concrete beams using artificial neural networks. Part II: beams with stirrups. *Eng Struct* 2004;26(7):927–36.
- [22] Mansour M, Ydicleli M, Lee JY, Zhang J. Predicting the shear strength of reinforced concrete beams using artificial neural networks. *Eng Struct* 2004;26(6):781–99.
- [23] Oreta AWC. Simulating size effect on shear strength of RC beams without stirrups using neural networks. *Eng Struct* 2004;26(5):681–91.
- [24] Flood I, Muszynski L, Nandy S. Rapid analysis of externally reinforced concrete beams using neural networks. *Comput Struct* 2001;79(17):1553–9.
- [25] Oreta AWC, Kawashima K. Neural network modeling of confined compressive strength and strain of circular concrete columns. *J Struct Eng* 2003;129(4):554–61.
- [26] Tang C, Chen H, Yen T. Modeling confinement efficiency of reinforced concrete columns with rectilinear transverse steel using artificial neural networks. *J Struct Eng* 2003;129(6):775–83.
- [27] Chao-Wei T, How-Ji C, Yen T. Modeling confinement efficiency of reinforced concrete columns with rectilinear transverse steel using artificial neural networks. *J Struct Eng* 2003;129(6):775–83.
- [28] Caglar N. Neural network based approach for determining the shear strength of circular reinforced concrete columns. *Construct Build Mater* 2009;23(10):3225–32.
- [29] Hola J, Schabowicz K. New technique of nondestructive assessment of concrete strength using artificial intelligence. *NDT&E Int* 2005;38(4):251–9.
- [30] Kavzoglu T, Mather PM. The use of backpropagating artificial neural networks in land cover classification. *Int J Remote Sens* 2003;24(23):4907–38.
- [31] Guven A, Gunal M. Prediction of local scour downstream of grade-control structures using neural networks. *J Hydraulic Eng* 2008;134(11):1656–60.
- [32] Guven A, Gunal M. Genetic programming approach for prediction of local scour downstream hydraulic structures. *J Irrigat. Drainage Eng* 2008;134(2):241–9.
- [33] Azamathulla HMD, Ghani AAB, Zakaria NA, Aytac Guven A. Genetic programming to predict bridge pier scour. *J Hydraulic Eng* 2010;136(3):165–9.
- [34] Vapnik VN. The nature of statistical learning theory. New York: Springer-Verlag; 1995.
- [35] Dibike YB, Velickov S, Solomatine DP, Abbott MB. Model induction with support vector machines: introduction and applications. *J Comput Civil Eng* 2001;15(3):208–16.
- [36] Pal M, Mather PM. Support vector classifiers for land cover classification. *Map India, New Delhi*, 28–31 January; 2003. <<http://www.gisdevelopment.net/technology/rs/pdf/23.pdf>>.
- [37] Gill MK, Asefa T, Kemblowski MW, Makee M. Soil moisture prediction using Support Vector Machines. *J Am Water Resources Assoc* 2006;42(4):1033–46.
- [38] Pal M, Goel A. Prediction of the end depth ratio and discharge in semi circular and circular shaped channels using support vector machines. *Flow Measur Instrum* 2006;17(1):50–7.
- [39] Pal M. Support vector machines-based modelling of seismic liquefaction potential. *Int J Numer Anal Methods Geomech* 2006;30(10):983–96.
- [40] Pal M, Goel A. Prediction of end-depth-ratio and discharge in trapezoidal shaped channels using Support Vector Machines. *Water Resource Manage* 2007;21(10):1763–80.
- [41] Pal M, Deswal S. Modelling pile capacity using support vector machines and generalized regression neural network. *ASCE J Geotech Geoenviron Eng* 2008;134(7):1021–4.
- [42] Pal M. Kernel methods in remote sensing: a review. *ISH J Hydraulic Eng (Special Issue)* 2009;15(1):194–215.
- [43] American Concrete Institute (ACI) Committee 318. Building code requirements for reinforced concrete. ACI 318-99 Commentary. ACI 318R-99, Farmington Hills, Michigan; 1999.
- [44] CEB-FIP MC90. CEB-FIP model code 1990, London, Thomas Telford; 1993.
- [45] Vapnik VN. Statistical learning theory. New York: John Wiley and Sons; 1998.
- [46] Smola AJ. Regression estimation with support vector learning machines. Master's thesis, Technische Universität München, Germany; 1996.
- [47] Cortes C, Vapnik VN. Support vector networks. *Mach Learn* 1995;20(3):273–97.
- [48] Luenberger DG. Linear and nonlinear programming. 2nd ed. Reading, Massachusetts: Addison-Wesley Inc.; 1984.
- [49] Tan KH, Kong FK, Teng S, Guan L. High-strength concrete deep beams with effective span and shear span variations. *ACI Struct J* 1995;92(37):395–405.
- [50] Smith KN, Vantsiotis AS. Shear strength of deep beams. *ACI Struct J* 1982;79(3):201–21.
- [51] Kong FK, Robins PJ, Cole DF. Web reinforcement effects on deep beams. *ACI Struct J* 1970;67(73):1010–7.
- [52] Teng S, Kong FK, Poh SP. Shear strength of reinforced and prestressed concrete deep beams. Part II: The supporting evidence. *Proc Inst Civil Eng Struct Build* 1998;128:124–43.
- [53] Tan KH, Lu HY, Teng S. Size effect in large prestressed concrete deep beams. *ACI Struct J* 1999;96(6):937–46.
- [54] Tan KH, Tong K, Tang CY. Direct strut-and-tie model for prestressed deep beams. *J Struct Eng* 2001;127(9):1076–84.
- [55] Marti P. Basic tools of reinforced concrete beam design. *ACI Struct J* 1985;82(4):46–56.
- [56] Schlaich J, Schafer K, Jennewein M. Towards a consistent design of structural concrete. *J Prestressed Concrete Inst* 1987;32(3):74–150.
- [57] Collins MP, Mitchell D, Adebare PE, Vecchio FJ. A general shear design method. *ACI Struct J* 1996;93(1):36–45.
- [58] Ramirez JA, Breen JE. Evaluation of a modified truss model approach for beams in shear. *ACI Struct J* 1991;88(5):562–71.
- [59] Tang CY, Tan KH. Interactive mechanical model for shear strength of deep beams. *J Struct Eng* 2004;130(10):1534–44.
- [60] Canadian Standards Association (CSA). Design of concrete structures: Structures (design)—a national standard of Canada. CAN-A23.3-94, Clause 11.1.2, Toronto; 1994.
- [61] Witten IH, Frank E. Data mining: practical machine learning tools and techniques. 2nd ed. San Francisco: Morgan Kaufmann; 2005.
- [62] Platt JC. Fast training of support vector machines using sequential minimal optimization. In: Schölkopf B, Burges C, Smola A, editors. *Advances in kernels methods: support vector machines*. Cambridge, MA: MIT Press; 1999.
- [63] Sung AH, Mukkamala S. Identifying important features for intrusion detection using support vector machines and neural networks. In: *Workshop on statistical and machine learning techniques in computer intrusion detection*, June 11–13, Johns Hopkins University, US; 2002.